UDC 535.15: 621.391: 535.016

Interference Refractometry of Terahertz Surface Plasmon-Polaritons Launched by a Free-Electron Laser

V. V. Gerasimov*, B. A. Knyazev†, A. K. Nikitin‡, V. V. Nikitin‡, T. A. Rijova§

* *Budker Institute of Nuclear Physics SB RAS*
Lavrentiev av. 11, Novosibirsk, Russia

† *Novosibirsk State University*
Pirogova str. 2, 630090 Novosibirsk, Russia

‡ *Scientific and Technological Center for Unique Instrumentation of RAS*
Butlerova str., 15, 117342 Moscow, Russia

§ *General Physics Department*
People's Friendship University of Russia
Miklukho-Maklaya str., 6, 117198 Moscow, Russia

The problem of terahertz (THz) surface plasmon-polaritons (SPP) refractometry, i.e. determination of their complex refractive index $\kappa = \kappa' + i \cdot \kappa''$ employing interferometric measurements, is considered in the paper. It is stated that one can determine both parts of κ provided the interference pattern formed by a reference bulk wave and the wave produced by the SPP is recorded. The idea was tested for SPP generated by monochromatic radiation (wavelength 140 μm) of Novosibirsk THz free-electron laser on gold samples covered with different thickness *ZnS* layers. Besides, intensity distribution of the SPP field in air over the track has been registered instantly with an uncooled vanadium oxide microbolometer focal plane array consisting of 320×240 sensitive elements. The results obtained are in good agreement with the theory provided the covering layer thickness is equal or exceeds 2 μm.

Key words and phrases: terahertz radiation, surface plasmon-polaritons, refractometry, surface electromagnetic waves, free-electron laser.

1. Introduction

Surface plasmon-polaritons (SPP) corresponding a complex of $p-$polarized electromagnetic wave and a wave of free charges induced by the former onto a conducting surface and propagating along the conductor-dielectric interface are widely used in optics for surface control [1].

SPP characteristics (propagation length L, phase velocity, and field penetration depth δ in air) are very sensitive to optical properties of the surface and its transition layer. Having determined the complex refractive index $\kappa = \kappa' + i \cdot \kappa''$ of the SPP, one can calculate two unknown parameters of the layer or optical constants of the surface. By analogy with optics of bulk materials the division of SPP science dealing with determination of κ may be called SPP refractometry. This concept is well developed for the visible and middle infrared (IR) spectral ranges [2], but not for the far IR range, specifically for the terahertz (THz) region (frequencies from 0.1 to 10 THz), where the SPP characteristics are very similar to those of a plane wave (with refractive index n) in air: the difference $(\kappa' - n) < 10^{-4}$, L amounts to meters, and δ reaches centimeters [3].

On the one hand these peculiarities complicate conversion of bulk THz radiation into SPP (efficiency of the process is inversely proportional to the wavelength λ and amounts only to hundredths of a percent for a bare metal surface in the THz range), but on the other hand they make it possible to reflect THz SPP like plane waves [4] and build interferometers in which radiation runs macroscopic distances in the form of

This study was supported by Russian Federal Special Program "Scientific, research and educational staff of innovation Russia"), contract number 14.B37.21.0732. The work was carried out with the involment of the equipment belonging to the Siberian Synchrotron and Terahertz Radiation Centre. The authors are cordially thankful to the NovoFEL team for their assistance in the experiments.

SPP [5]. From this point of view free-electron lasers (FEL) are the best candidates as sources of THz radiation in such interferometers until an effective way of bulk radiation conversion into SPP is found [6]. Besides, use of FELs in THz SPP interferometers is reasonable as their beam power can reach nowadays hundreds of Watts that partially compensates the low transformation efficiency, while the ability of FELs to tune their radiation frequency meets the case of spectroscopic measurements [7].

In this paper we describe our experiments aimed at creation of a Mach–Zehnder interferometer employing monochromatic THz SPP propagating in one of the shoulders. The interference pattern recorded while the distance run by the SPP is being changed comprises information about the real κ' as well as about the image κ'' part of the SPP refractive index. That is why interferometric measurements make it possible to perform refractometry of THz SPP, otherwise – refractometry of conducting surfaces, which is impossible to do by any other optical method in view of high reflectivity of metals at THz frequencies.

2. Foundations of the Method

The principle idea of interferometric SPP refractometry was first put forward by Prof. G.N. Zhizhin and coworkers in paper [8]. It was noted that information about κ' and κ'' values was stored in the interference pattern formed by two bulk waves (the reference one and the wave produced by the SPP due to its diffraction on the sample edge) recorded by photodetector array 3 disposed in the plane of incidence at a distance b from the edge and normally to the SPP track (Fig. 1). However, accuracy of this method was found to be insufficient as the beams interfere at a large angle, making the period of the pattern comparable with the wavelength.

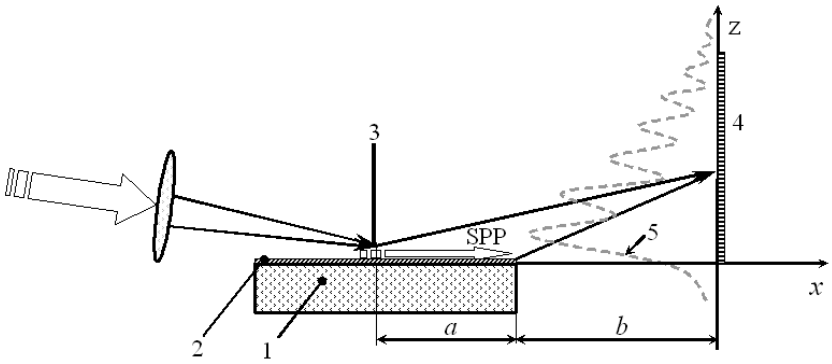

Figure 1. Schematic of the first infrared SPP interferometer: 1 — metal sample; 2 — layer under study; 3 — screen with its edge spaced from the sample surface by a distance of about 10λ; 4 — detector array; 5 — registered interferogram [8]

As it was noted above, SPP at THz frequencies can be treated in many respects like plane waves as their field penetrates into air to a distance of several centimeters. On the other hand, the process of THz SPP excitation on a plane surface by means of incident radiation is attended by an unavoidable production of phantom bulk waves (BWs), overlapping with the SPP field [9]. We integrated these peculiarities of THz SPP and suggested a simpler and more effective scheme of a SPP interferometer functioning in parallel beams one of which is the SPP itself, while the other is a bulk radiation produced on the coupling element converting light into SPP (Fig. 2) [10].

The interferometer functions as follows. By mirrors 2 and 3, radiation of source 1 is directed towards the edge of screen 5, spaced from sample 4 by a controllable distance. Due to diffraction the radiation is partially transformed into SPP and BWs, propagating at various angles from the surface. Among this set of BWs there is a

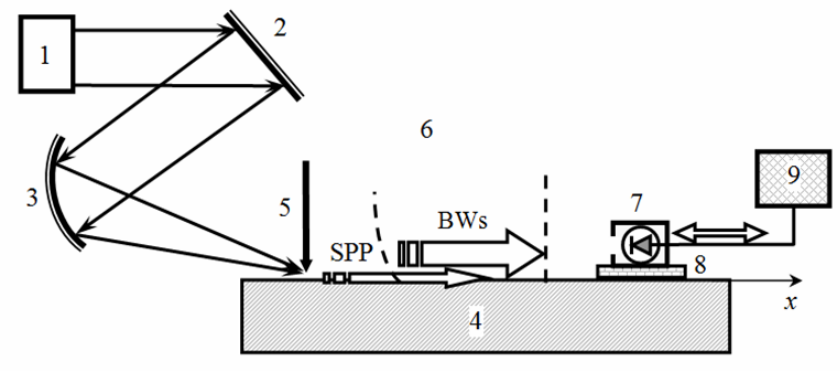

Figure 2. Scheme of SPP spectrometer employing interaction of surface and bulk waves: 1 – tunable source of THz monochromatic radiation; 2 – mirror; 3 – focusing mirror; 4 – sample; 5 – screen with its edge spaced from the sample surface by a distance of about 10λ; 6 – surrounding medium (air); 7 – photo detector placed on the platform 8, moving along the sample surface; 9 - data-handling unit.

BW whose wave vector is parallel to the surface while its field invariably overlaps with the SPP field. The BW and SPP run along the surface with different phase velocities since κ' is larger than the BW refractive index n. As a result of the Joule loses, the SPP intensity decreases exponentially with the absorption factor $\alpha{=}2k_o \cdot \kappa''$ (here $k_o{=}2\pi/\lambda$). Having run the same distance x, the BW and SPP acquire phase shift $\Delta\varphi = k_o x \cdot (\kappa' - n)$ and meet detector 7. Being coherent, the BW and SPP interfere and illuminate the detector sensitive element with the intensity I described by the expression:

$$I(x) = I_1 + I_o \cdot \exp(-\alpha \cdot x) + 2 \cdot \sqrt{I_1 \cdot I_o \cdot exp\,(-\alpha \cdot x)} \cdot \cos(\Delta\phi)\,, \tag{1}$$

here I_1 is the BW intensity, independent on the distance x (supposing that air does not absorb the radiation); I_o is the SPP intensity right under screen 5 when $x = 0$.

The interference pattern (interferogram) registered by mobile detector 7 is characterized by a constant period Λ. On measuring Λ, one can estimate value of the SPP refractive index from the evident formula:

$$\kappa' = n + \lambda/\Lambda. \tag{2}$$

The absorption index κ'' of the SPP can be calculated by putting the SPP intensity values measured in two different maxima of the interferogram I_{m1} and I_{m2} in the following formula (its derivation one can find in Appendix):

$$\kappa'' = \frac{2 \cdot \ln\left(\frac{\sqrt{I_{m1}}-\sqrt{I_1}}{\sqrt{I_{m2}}-\sqrt{I_1}}\right)}{k_o \cdot (x_2 - x_1)}, \tag{3}$$

here x_1 and x_2 are the coordinates of corresponding maxima, $x_2 > x_1$.

On putting the found values of κ' and κ'' in the SPP dispersion equation for a three-layer structure [2], unit 9 computes two parameters of the structure: the complex dielectric permittivity ε of the metal surface or its transition layer (or the layer thickness and its material refractive index). Note that the contrast of the interferogram can be controlled by changing the distance from the screen edge to the sample surface.

To illustrate the technique of THz SPP amplitude-phase refractometry in parallel surface and bulk beams let us consider the following example. Suppose we have to determine the dielectric permittivity of aluminum (Al) at $\lambda = 100\,\mu$m employing the

method. To reduce L below 30 cm (reasonable size of the table-top sample) let's cover the metal surface with a uniform 0.7 μ m germanium (Ge) layer thick. Assume that the screen converting the incident radiation into SPP is spaced from the surface by the distance ensuring equality $I_1 = I_o$, i.e. intensity of the BW propagating parallel to the surface equals intensity of the SPP right under the screen. The surrounding medium is air ($n = 1.00027$).

Calculated interferogram $I(x)$ for this case is depicted in Fig. 3. The calculations were carried out using the Drude model for dielectric permittivity of metals, assigning that the plasma frequency and the frequency of free electron collisions for Al were equal to 660 cm^{-1} and 119000 cm^{-1}, accordingly [11].

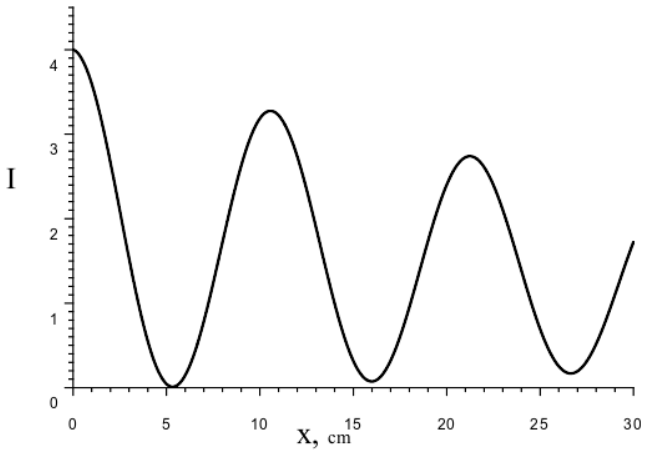

Figure 3. Interferogram for the structure "Al –Ge layer 0.7 μm thick - Air" at $\lambda = 100\mu$m

Having registered the interferogram by detector 7, one can determine both κ' and κ''. For example, from the graph presented it follows that: 1) the interferogram period $\Lambda = 10.675$ cm, which according to (2) corresponds to $\kappa' = 1.00121$; 2) the resulting intensities in the first I_{m1} and the second I_{m2} maxima, reached at the distances $x_1 = 10.565$ cm and $x_2 = 21.240$ cm, are equal to 3.275 and 2.739 accordingly. Putting the values of I_{m1}, I_{m2}, x_1 and x_2 in (3), we got $\kappa'' = 6.3 \cdot 10^{-5}$. At the final stage of the execution procedure the SPP dispersion equation for a three-layer structure can be solved relatively to ε_{Ge}. Thus in the example considered we obtained that Ge permittivity at λ=100 μm is equal to $\varepsilon_{Ge} = 16 + i \cdot 0.008$. Having done similar measurements and calculations for other λ one can determine ε_{Ge} in the whole THz range.

3. Experimental setup

The most acute problem in developing THz SPP techniques is efficient excitation of SPP. To convert bulk radiation into SPP one has to match their phase velocities and the tangential components of the wave vectors. In the visible range these conditions could be met using a diffraction grating formed on the metal surface or a prism made of a material optically denser than the environment (the attenuated total reflection (ATR) method). However in the IR and far IR ranges, the ATR method does not work as the introduction of a prism into the SPP field changes the waveguiding structure so much that the incidence angle corresponding to the optimum conditions of SPP excitation becomes smaller than the critical one. That is why the only opportunity to excite THz SPP by bulk radiation on a plane surface is diffraction of the latter on an object placed within the SPP field in air.

The experiments were performed employing radiation with $\lambda = 140\,\mu$m at the Novosibirsk FEL (NovoFEL) generating a continuous train of 100-ps pulses with a

repetition rate of 5.6 MHz, the average power of the radiation at the user stations being around hundred Watts, the radiation angular divergence - $3{\cdot}10^{-3}$ radians [7]. The samples represented themselves 10 mm thick, 35 mm wide and 150 mm long plane-parallel glass plates with optically polished top surface covered with a nontransparent thermally evaporated 1 μm thick gold film covered with a zinc-sulfide (ZnS, refractive index equals 3.4) layer of various thickness. Measurements were performed in the air atmosphere with the absorption coefficient $\alpha = 2k_o k_2 = 0.173\, m^{-1}$ (here k_2 is the absorption index of air) at $\lambda = 140\,\mu$m.

The intensity of the SPP field was measured by an uncooled vanadium oxide microbolometer focal plane array (MBFPA) consisting of 320 × 240 sensitive elements (common size - 16×12 mm^2), made at the Rzhanov Institute of Semiconductor Physics (SB RAS, Novosibirsk) [12]. The MBFPA was applied to direct recording "terahertz video" with frequency up to 90 Hz.

Fig. 4 sketches the device we used in the experiments. FEL radiation, modulated with frequency of 15 Hz by shutter 1, arrived on wire polarizer P_1 carrying out the function of a regulator of capacity of the radiation intensity submitted to the working station.

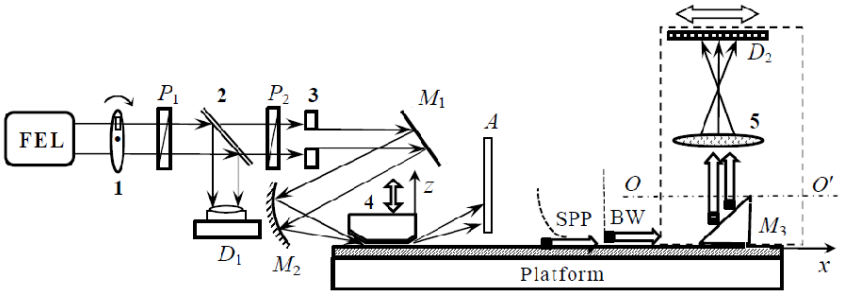

Figure 4. Schematic of the setup for monochromatic THz SPP refractometry. Designation interpretations see in the text

For accounting the intensity variations a portion of the radiation was permanently reflected by splitter 2 onto pyroelectric receiver D_1. Polarizer P_2 was used to control polarization of the radiation. Further $p-$polarized radiation passed through 10 mm iris diaphragm 3. To prevent parasitic flares the diaphragm was built in a big foam screen. On reflecting from flat mirror M_1, the beam was focused by cylindrical mirror M_2 (focal length – 70 mm) on element 4 converting FEL radiation into SPP. The element was elaborated by Prof. D. Grischkowsky and coworkers and is characterized by relatively high transformation efficiency (depending on thickness of the dielectric layer covering the surface) [13]. The element represented itself a bar (prism) with two axial cuts of the lower facet (40 × 40 mm^2 top base and the 20×40 mm^2 bottom base; the cut angles of the bottom base were 20^o and 8^o for the entry and exit mouths, accordingly). Both the cuts and the facet were covered with a nontransparent gold film. Distance (gap) h between the prism and the sample (dashed box) was regulated by a micrometer with accuracy of 10 microns. The metallized base of the prism brought at distance $h \approx \lambda$ to the sample surface formed a waveguide able to lead modes of TM type. These modes (the single-mode regime – preferable) diffracted at the exit mouth of the element and partially converted into SPP. The diffracted bulk waves were blocked by absorber A, while the SPP slipped under it.

Calculations, made employing computer program Ansoft HFSS (tm) v12.0 [14], have shown that the bulk wave radiation pattern formed at the output of prism 4 depends on the diffracting waveguide mode structure in the following manner: in the single-mode regime, when only TM_0-mode, having no cut-off in value of h, exists in the gap, the pattern is very narrow and is directed practically along the sample surface; in a multimode regime, when $h > \lambda/2$ the pattern has several maxima directed away from the sample surface. Therefore to insure co linearity of the SPP and the reference

beam as well as intensity permanency of the last-named in the near-surface region all along the SPP track the gap size h should be chosen smaller than $\lambda/2$.

Having passed distance x, the SPP and the BW propagating along the sample surface, ran on the mobile 15 mm high plane mirror M_3 with its reflecting face inclined at angle of 45°to the surface. Due to interaction with the mirror the SPP received a negative (relatively to the direction of propagation) impulse that led to a decrease of the SPP wave vector to a value less than that of a plane wave in air, which was sufficient for SPP conversion into a BW. Interference of this BW with the BW produced at the output mouth of prism 4 and reflected by mirror M_3 was registered by microbolometer focal-plane array (MBFPA) D_2. Employment of the array made it possible not only to estimate the resulting intensity of the interfering beams, but to monitor its distribution over the sample surface as well.

To change the distance run by the SPP mirror M_3, together with focusing lens 5 and MBFPA, was mounted onto a computer-controlled horizontally moving platform. The interfering beams were focused at the MBFPA by TPX (polymethylpentene) lens 5 with focal distance f=5 mm, while the distance from the upper edge of mirror M_3 to the lens was 175 mm and the distance from the lens to the microbolometer array was 70 mm, that resulted in 2.5 image reduction as compared with the SPP field real size on mirror M_3. Thus, MBFPA registered a reduced distribution of the interference pattern intensity, located at level of the upper edge (plane OO') of mirror M_3 and oriented parallel to the surface of the sample. Note, that one should not change the SPP run-distance by moving prism 4 as it may lead to variations of the FEL radiation-SPP conversion efficiency while recording the interferogram.

4. Experimental results and their discussion

The experiments were performed on the described above setup with samples containing bare gold surface or gold covered with 1, 2 or 3 μm thick ZnS layer.

As an example, the image of the intensity distribution in plane OO$\prime$, registered by the MBFPA after the SPP have run 110 mm along the sample with 3 μm thick ZnS layer on its top, is presented (being magnified by 2.5 times) in Fig. 5. The gap size h was 120 μm. By the vertical dashed line the approximate position of the sample surface is traced. Flare of MBFPA pixels observed to the left of this line are present, to our mind, due to the SPP diffraction on mirror M_3 edge adjoining the sample surface. The right part of the frame illustrates the resulting intensity of the interference pattern. The upper embedding depicts the dependence of the relative resulting intensity on the distance spacing points of mirror M_3 from the sample surface in the plane of SPP track.

To plot the experimental dependencies of the relative resulting intensity I_{rel} on distance x run by the SPP we integrated signals from all MBFPA pixels disposed against mirror M_3 edge in the area enclosed by the rectangle $1.28 \times 2.55\ mm^2$ as it is shown in Fig. 5. Besides, the background signal (when the radiation on the outlet of prism 4 was trapped) was subtracted from the measured one and the resultant signal was normalized to the corresponding one from receiver D_1, thus obtaining relative signal I_{rel} for a given distance x. The error of measurements caused by discrepancy of mirror M_3 installation and possible variations in values of gap h did not exceed 10 %.

On executing in this way images similar to that presented in Fig. 5 and obtained at various distances x we have plotted experimental graphs $I_{rel}(x)$ for the samples with 2 and 3 μm thick ZnS covering layers (dashed lines in Figs. 6 and 7).

By means of program Origine-8 and employing the experimental points and expression (1) we executed approximation dependences $I_{rel}(x)$, while quantities I_0, I_1 and L were used as fitting parameters (solid lines in Figs. 6 and 7). From these graphs one can see that better correlation of the approximating curves with the results of measurements is reached for larger distances x, when parasitic flare of the MBFPA by BWs, propagating at an angle to the surface, is essentially weakened. The larger was gap h between prism 4 and the sample (or, to be more exact, with transition from the

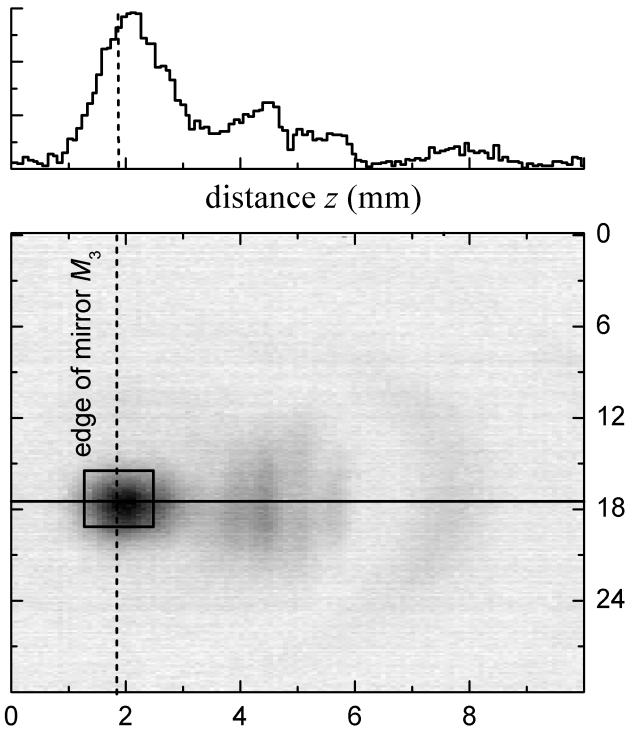

Figure 5. Frame of the SPP field intensity distribution near mirror M_3 edge adjoining the sample surface recorded by microbolometer array D_2 when the SPP had run 110 mm along the gold sample with 3 μm thick ZnS layer on its top. The estimated signal was integrated over the area enclosed by the black rectangle 1.28×2.55 mm^2

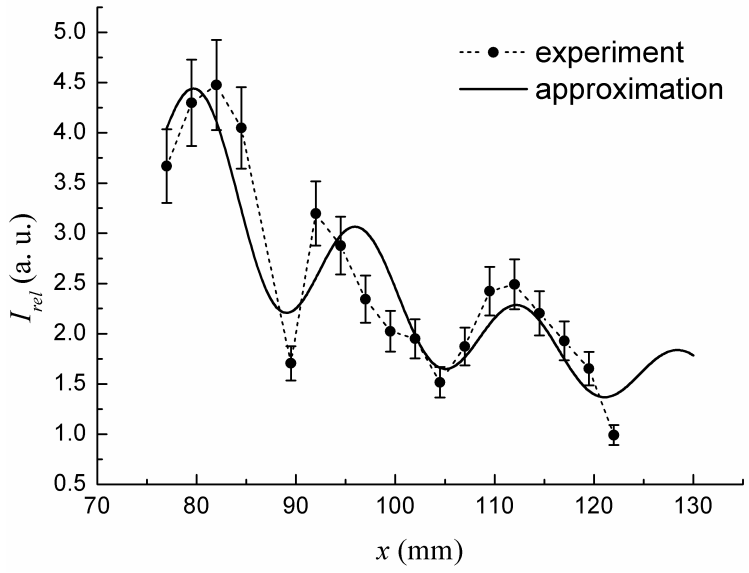

Figure 6. Dependence of the relative signal I_{rel} registered by microbolometer array D_2 upon distance x run by the SPP along the gold sample with 2μm thick ZnS layer on its top. The aria of signal integration is $[0.64 \times 2.55]$ mm^2

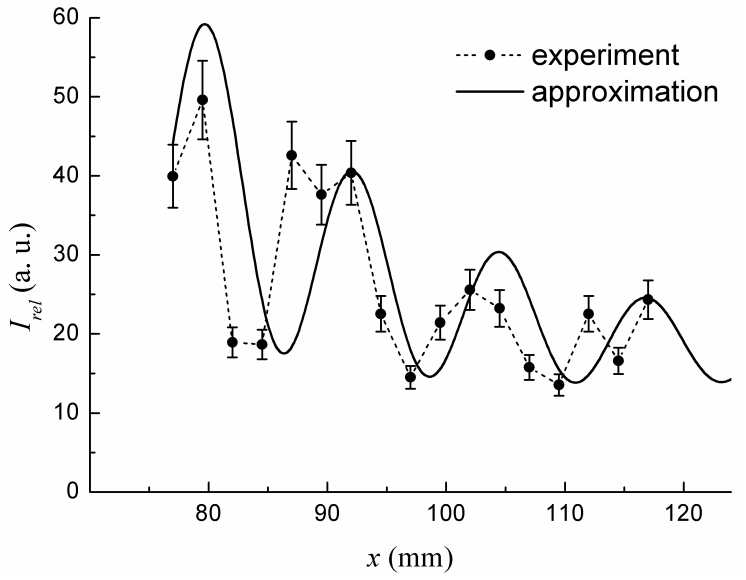

Figure 7. Dependence of the relative signal I_{rel} registered by microbolometer array D_2 upon distance x run by the SPP along the gold sample with 3 mu m thick ZnS layer on its top. The aria of signal integration is $[1.28 \times 2.55]$ mm^2.

single-mode to a multimode regime in the waveguide) the worse was the correlation at small x.

Note that the larger is thickness d of the covering layer the smaller is period Λ of the interference pattern, that indicates an increase of the real part κ' of the SPP refractive index. On the other hand the SPP attenuation is proportional to the layer thickness too, that is indicated by greater slope of the pattern in the case of larger.

Having determined periods Λ of these approximated interference patterns we calculated, by formula (2), real parts κ' of the corresponding SPP refractive indexes. On substituting intensity maxima values and their coordinates in formula (3) the SPP propagation lengths L along the samples were estimated and used afterwards for corresponding values of the SPP refractive indexes imaginary parts calculations: $\kappa'' = (2k_0L)^{-1}$.

Results of the calculations are presented in Table 1. Values of the correlation factor R characterizing the degree of deviations of the approximation curves from the results of measurements are placed in the extreme right column of the Table.

Table 1

Results of calculations

Sample	Λ, mm	L, mm	κ'	κ''	Correlation factor R
$Au + ZnS$, 2μm	16.0 ± 0.5	26	1.0091 ± 0.0003	4.3×10^{-4}	0.788
Au + ZnS, 3 μm	12.3 ± 1.7	17	1.0112 ± 0.0016	6.6×10^{-4}	0.742

Similar measurements executed for bare gold and containing ZnS layer with thickness less than 2.0 microns have shown that in this case patterns period was much smaller as compared with the limits of distance x run by the SPP, which did not exceed 50 mm in the experiments performed.

5. Conclusion

The interferometric method and the device for determining complex refractive index of monochromatic terahertz surface plasmon-polaritons have been developed, though the device has to be refined. The method and the interferometer may be used not only for refractometry of real conducting surfaces at terahertz frequencies, but for sensor applications and thin layer spectroscopy as well. Moreover, provided the source of light is a broad-band one the developed technique may be employed for performing Fourier-spectroscopy of thin samples and metal surfaces in the terahertz spectral range.

6. Appendix

Suppose we have measured intensity I_{m1} and I_{m2} in two maxima of the interference pattern corresponding to distances x_1 and x_2 run by the SP. With regard to the fact that for maxima $\Delta\varphi = 2\pi b$ (here b – is an integer) these intensities, in accordance with formula (1), may be described as follows:

$$I_{m1} = I_1 + I_{21} + 2\sqrt{I_1 \cdot I_{21}} \text{ and } I_{m2} = I_1 + I_{22} + 2\sqrt{I_1 \cdot I_{22}},$$

here I_1 – is intensity of the bulk wave, I_{21} and I_{22} – are intensities of the SPP at coordinates x_1 and x_2, respectively.

Solving these equations relatively I_{21} and I_{22} we get: $I_{21} = \left(\sqrt{I_{m1}} - \sqrt{I_1}\right)^2$ and $I_{22} = \left(\sqrt{I_{m2}} - \sqrt{I_1}\right)^2$. In view of the exponential character of SPP field decay we can express I_{22} through I_{21} on assumption that $x_1 < x_2 : I_{22} = I_{21} \cdot \exp(-\alpha \cdot \Delta x)$, here $\alpha = k_o \cdot \kappa''$ – is the SPP absorption coefficient, $\Delta x = x_2 - x_1$. Wherefrom it follows that: $\alpha \cdot \Delta x = ln\,(I_{21}/I_{22})$. Substituting the expressions for I_{21}, I_{22} and α in the last equation we get the required formula (3).

References

1. *Maier S. A.* Plasmonics: Fundamentals and Applications. — Springer, 2007. — 223 p.
2. Surface polaritons. Surface electromagnetic waves at surfaces and interfaces / Ed. by V. M. Agranovich, D. L. Mills. — Amsterdam, N.-Y., Oxford, 1982. — 587 p.
3. *Knyazev B. A., Kuzmin A. V.* Surface electromagnetic waves: from visible range to microwaves // Bulletin of Novosibirsk State University (Physics). — 2007. — Vol. 2(1). — Pp. 108–122.
4. Two-dimensional optics with surface electromagnetic waves / R. J. Bell, C. A. Goben, M. Davarpanah et al. // Applied Optics. — 1975. — Vol. 14 (6). — Pp. 1322–1325.
5. Dispersive Fourier-transform spectroscopy of surface plasmons in the Infrared Frequency Range / G. N. Zhizhin, A. P. Kiryanov, A. K. Nikitin, O. V. Khitrov // Optics and Spectroscopy. — 2012. — Vol. 112, No 4. — Pp. 545–550.
6. First experiments on application of free-electron laser terahertz radiation for optical control of metal surfaces / G. D. Bogomolov, U. Y. Jeong, G. N. Zhizhin et al. // J. of Surface Investigation. X-ray, Synchrotron and Neutron Techniques. — 2005. — No 5. — Pp. 57–63.
7. *Knyazev B. A., Kulipanov G. N., Vinokurov N. A.* Novosibirsk terahertz free electron laser: instrumentation development and experimental achievements // Measurement Science and Technology. — 2010. — Vol. 21. — 054017.
8. IR surface plasmon (polariton) phase spectroscopy / V. I. Silin, S. A. Voronov, V. A. Yakovlev et al. // Intern. J. Infrared & Millimeter Waves. — 1989. — Vol. 10(1). — Pp. 101–120.

9. Method for identifying diffraction satellites of surface plasmons in terahertz frequency range / V. V. Gerasimov, B. A. Knyazev, A. K. Nikitin, V. V. Nikitin // Technical Physics Letters. — 2010. — Vol. 36(11). — Pp. 1016–1019.
10. Surface plasmon dispersive spectroscopy of thin films at THz frequencies / A. K. Nikitin, O. V. Khitrov, A. P. Kyrianov et al. // Proc. SPIE. — 2010. — Vol. 7376. — 73760U.
11. Optical properties of the metals Al, Co, Cu, Au, Fe, Pb, Ni, Pd, Pt, Ag, Ti and W in the infrared and far infrared / M. A. Ordal, L. L. Long, R. J. Bell et al. // Applied Optics. — 1983. — Vol. 22(7). — Pp. 1099–1119.
12. Microbolometer detector arrays for the infrared and terahertz ranges / M. A. Dem'yanenko, D. G. Esaev, V. N. Ovsyuk et al. // J. Optical Technology. — 2009. — Vol. 76(12). — Pp. 739–743.
13. *Jeon T.-I., Grischkowsky D.* THz Zenneck surface wave (surface plasmon) propagation on a metal sheet // Applied Physics Letters. — 2006. — Vol. 88. — 061113.
14. `http://www.ansoft.com`.

УДК 535.15: 621.391: 535.016

Интерференционная рефрактометрия терагерцовых поверхностных плазмон-поляритонов, генерированных лазером на свободных электронах

В. В. Герасимов[*], **Б. А. Князев**[†], **А. К. Никитин**[‡], **В. В. Никитин**[‡], **Т. А. Рыжова**[§]

[*] *Институт ядерной физики им. Г. И. Будкера СО РАН*
Новосибирск, 630090, Россия

[†] *Новосибирский государственный университет*
ул. Пирогова д.2, 630090 Новосибирск, Россия

[‡] *Научно-технологический центр уникального приборостроения РАН*
117342 Москва, Россия

[§] *Кафедра общей физики*
Российский университет дружбы народов
ул. Миклухо-Маклая, 6, Москва, 117198, Россия

В статье рассмотрена проблема интерференционной рефрактометрии монохроматических терагерцовых (ТГц) поверхностных плазмон-поляритонов (ППП), т.е. задача определения их комплексного показателя преломления $\kappa = \kappa' + i \cdot \kappa''$. Показано, что интерференционная картина, полученная в результате взаимодействия опорного пучка объёмного излучения и объёмной волны, порождаемой ППП, содержит информацию об обеих частях κ. Метод апробирован для ППП, генерируемых излучением Новосибирского лазера на свободных электронах (длина волны 140 мкм) на поверхности золотых образцов с ZnS покрытием различной толщины. Кроме того, с помощью неохлаждаемой матрицы (320×240 пикселей) микроболометров на основе окиси ванадия получены изображения распределения интенсивности поля в воздухе над треком ППП. Результаты измерений хорошо согласуются с расчётными для покровного слоя толщиной 2 мкм и более.